Tree Physiology 26, 285–301

Simulation of effects of wood microstructure on water transport

CRAIG A. AUMANN[1,2] and E. DAVID FORD[3]

[1] *Department of Biological Sciences, University of Alberta, Edmonton AB, T6G 2E9, Canada*

[2] *Corresponding author (caumann@ualberta.ca)*

[3] *College of Forest Resources, University of Washington, Seattle, WA 98195, USA*

Received June 18, 2003; accepted June 11, 2005; published online December 15, 2005

Summary A tracheid-level model was used to quantify the effects of differences in wood microstructure between coastal and interior Douglas-fir (*Pseudotsuga menziesii* (Mirb.) Franco var. *menziesii* and var. *glauca*) wood on larger scale properties like hydraulic conductivity. The model showed that tracheid length, the ease of flow through a bordered pit and effective tracheid diameter can all limit maximum hydraulic conductivity. Among the model parameters tested, increasing bordered pit conductivity and tracheid length resulted in the greatest increase in maximum conductivity in both the inland and coastal ecotypes. A sensitivity analysis of the uncertainty between parameters governing flow through the bordered pit and air-seeding potential showed that, although decreased pit flow resistance increased maximum hydraulic conductivity, increased cavitation led to lower conductivity over time. The benefits of increasing the number of bordered pits depended on the intensity of the meteorological driving function: in drier environmental conditions, wood with fewer pits was more conductive over time than wood with more pits. Switching the bordered pit characteristics between coastal and interior wood indicated that the conductivity time course of coastal and interior wood was primarily governed by differences in the number of bordered pits and not differences in tracheid dimensions. The rate at which tracheids refilled had little effect on the conductivity time course of either coastal or interior wood during the first two summers when the wood was highly saturated, but had a marked influence in subsequent years once the cavitation profile stabilized. Our work highlights the need for more empirical work on bordered pits to determine whether variation in their number and properties is related to changing environmental conditions. In addition, a detailed simulation model of a bordered pit is needed to understand how variation in pit properties affects the relationship between ease of flow through a bordered pit and its potential for facilitating air-seeding.

Keywords: bordered pit, cavitation, Douglas-fir, hydraulic conductivity, refilling, tracheid dimensions.

Introduction

Differences in wood microstructure among tree species are thought to be a result of natural selection (Carlquist 2001), possibly to optimize mechanics, hydraulic conduction and photosynthesis in diverse environments (Tyree et al. 1994). Although this seems to be a consensus, only a few studies (e.g., Becker et al. 2003, Hacke et al. 2004, Sperry and Hacke 2004) have attempted to link large-scale properties of sapwood (e.g., hydraulic conductivity, saturation, or rates of cavitation) to wood microstructure attributes such as cell dimensions, number of bordered pits or the flow resistance of a single pit.

In this study, a model of coniferous wood microstructure is used in which cell and tissue attributes can be varied and large-scale sapwood properties predicted. The modeling approach allowed single or a small number of microstructure features to be altered while keeping others constant, thereby helping us to understand the effects of each feature individually. It also allowed us to apply identical sets of driving conditions to different wood microstructures. The model includes both tracheids and rays containing bordered pits. A block of $45 \times 45 \times 45$ interconnected tracheids is subjected to a pressure time course over which individual tracheids are allowed to cavitate in response to nucleation events or air-seeding and to refill. To avoid boundary influences, variables of interest are computed over a block of $29 \times 29 \times 29$ tracheids contained within the larger $45 \times 45 \times 45$ block.

We focused on the effects of the well-documented variation in the contrasting microstructures of coastal and interior Douglas-fir (*Pseudotsuga menziessii* (Mirb.) Franco var. *menziesii* and var. *glauca*) and variation in the driving conditions of water transport between coastal and interior regions. We summarize known variations in macroscale properties and wood microstructure between coastal and interior Douglas-fir, develop specific questions about how microstructure and driving conditions are related and then describe the model and environmental conditions assumed in our analysis. Our results show how microstructure influences large-scale water transport properties under alternative driving conditions and identify aspects of the microstructure that need further research.

The sapwood of Douglas-fir

Macroscale properties

In general, coastal Douglas-fir is more prone to drought stress

than interior Douglas-fir. The xylem of 3-year-old coastal Douglas-fir seedlings from wet and dry sites cavitates at higher water potentials than the xylem of interior seedlings from wet or dry sites (Kavanagh et al. 1999) and 5- and 16-month-old seedlings from coastal sites are less drought resistant than seedlings from interior sites (Ferrell and Woodward 1966, Pharis and Ferrell 1966). Minimum predawn water potentials observed over a season are lower in interior trees than in coastal trees (Lopushinsky 1986, Bauerle et al. 1999). Finally, the hydraulic conductivity of coastal wood is greater than that of interior wood (Miller 1969, Bramhall and Wilson 1971, Siau 1995).

Differences in wood microstructure

A summary of differences between coastal and interior wood is given in Table 1. Relative to coastal tracheids, interior tracheids are shorter and have smaller radial and tangential diameters. The smaller tracheid dimensions in interior wood than in coastal wood result in a greater number of tracheids per mm^2 cross section: 413 tracheids per mm^2 in coastal earlywood versus 533 in interior earlywood (Meyer 1971). The percentage of latewood in interior wood is also less than in coastal wood (~20 versus ~40%). Coastal wood has more pits per tracheid than interior wood (Meyer 1971), although properties of pit aperture radius and pit torus radius do not appear to differ (Krahmer 1961), and never-dried coastal sapwood has less pit aspiration than never-dried interior sapwood (Griffin 1919, Meyer 1971).

In conifers, latewood tracheids generally have thicker walls than earlywood tracheids (Jane 1956, p 81; Esau 1965, p 252) and the margo fibrils are denser in latewood pits than in earlywood pits (Esau 1965, p 252; Bauch et al. 1972, Figures 2–4). Although tracheid dimensions are known to vary with height and distance from the pith (Lee et al. 1916, Bannan 1964, Panshin and de Zeeuw 1980), little is known about how tracheid dimensions, number and attributes of bordered pits co-vary within Douglas-fir and its ecotypes or within conifers generally.

Water movement, cavitation and refilling

Water is transported to foliage under tension, which draws water through bordered pits in the uncavitated tracheids, forming the transpiration stream. The mechanisms by which a tracheid cavitates ensures that much of the water within that tracheid is transported away by the transpiration stream before the bordered pits are aspirated by the receding meniscus (Hart and Thomas 1967). Water remaining in the cavitated tracheid following pit aspiration (i.e., residual water) is a source of water in larger trees (Phillips et al. 2003). Under large tensions there is a large pressure gradient between the residual water in contact with the cavitated tracheid's wall and neighboring uncavitated tracheids that are part of the transpiration stream. The cell walls of tracheids are slightly permeable (Bailey and Preston 1969, Palin and Petty 1981, 1983) and the residual water is drawn out according to Darcy's law for saturated flow.

The water content of Douglas-fir sapwood changes seasonally (Chalk and Bigg 1956, Waring and Running 1978, Borghetti and Vendramin 1987), increasing in autumn and winter after summer drying, suggesting that a refilling mechanism operates. Two mechanisms have been suggested for refilling cavitated tracheids: (1) transport of water from developing cells in the phloem, cambium and immature xylem (PCIX) (Milburn 1975, 1979, 1996); and (2) active secretion through ray parenchyma (Holbrook and Zwieniecki 1999), possibly in-

Table 1. Summary of differences in microstructure between coastal and interior Douglas-fir.

Property	Coastal	Interior	Sources
Tracheid length (mm)	4.0–5.9	3.0–3.6	Lee et al. (1916), Bannan (1964)
Earlywood and latewood tangential width (μm)	34–45	31–34	Lee et al. (1916), Bannan (1964), Spicer and Gartner (2001)
Radial width (μm)			
Earlywood	40–56	36–41	Lee et al. (1916), Bannan (1964)
Latewood	~18	~18	
Cell-wall thickness (μm)			
Earlywood	~4	~4	Lee et al. (1916), Cote (1967)
Latewood	~8	~8	
% Latewood	~40	~20	Bannan (1964)
% Ray volume	~7	~7	Panshin and de Zeeuw (1980, Table 4.2)
No. bordered pits per tracheid			
Earlywood	~144	~65	Griffin (1919), Krahmer (1961), Meyer (1971)
Latewood			
Pit aperature radius (μm)	~2.8	~2.8	Krahmer (1961), Cote (1967, Pl. 11)
Pit torus radius (μm)	~6	~6	Krahmer (1961), Cote (1967, Pl. 11)
Hydraulic conductivity (10^{-5} m s^{-1})			Markstrom and Hann (1972), Siau
Wood	~5	~2	(1995), Spicer and Gartner (2001),
Earlywood	~7.3	–	Domec and Gartner (2002*b*), Bramhall
Latewood	~6.4	–	and Wilson (1971)

volving extraction of water by the parenchyma from elsewhere in the sapwood during periods of low xylem tension.

Questions to be answered with model simulations

On the basis of the Hagen-Poiseuille equation (e.g., Siau 1995) it has been argued that in fully saturated wood more water will flow through larger diameter earlywood tracheids than smaller diameter latewood tracheids (Tyree et al. 1994). The greater maximum conductivities of coastal wood relative to interior wood and the higher proportion of larger diameter earlywood tracheids relative to smaller diameter latewood tracheids (Domec and Gartner 2002*a*) is consistent with such predictions even if the explanation ignores the number of bordered pits per tracheid and the resistance offered by each pit (Tyree and Ewers 1991, Tyree et al. 1994). In addition, attributes that increase mean conductivity over time under particular environmental conditions may lead to lower conductivities under different environmental conditions. For example, more bordered pits may increase mean conductivity under one set of environmental conditions, yet result in lower mean conductivities under more severe environmental conditions because of increased cavitation. Thus, we posed two questions. (1) How do maximum conductivity and the conductivity time course change when the meteorological driving function, number and conductive properties of bordered pits, tracheid dimensions (length, diameter, effective diameter), tracheid refilling rates and proportion of latewood are altered? (2) Given the differing effects of altering tracheid microstructure on conductivity (and also mechanics), which microstructure features may have been the focus of natural selection?

Tracheid model

Our model is based on the tracheid model of Aumann and Ford (2002*b*) where the physical processes of water flow, tracheid cavitation, refilling, pit aspiration, pit de-aspiration and flow through the tracheid cell wall are described in detail. To answer the questions we posed, the model was altered by adding ray cells, allowing different tracheid dimensions in earlywood and latewood, changing the rules governing air-seeding and incorporating lumen flow resistance within tracheids and rays. These modifications are described below. Default parameter values used are specified in Table 2.

Table 2. Summary of parameter values for the coastal and interior wood models. The side length of a square ray cell is 10 µm. Earlywood cell wall thickness is 4 and 8 µm in latewood. Cell wall hydraulic conductivity is 2.25×10^{-19} m s^{-1}. The number of tracheids connected to each ray tracheid ranges from 2 to 4. The dynamic viscosity of water (µ) is 1×10^{-3} kg m^{-1} s^{-1} and the density of water (ρ) is 1000 kg m^{-3}. Abbreviations: REV = representative elementary volume; and K_p = bordered-pit flow constant.

Parameter	Sub-parameter	Coastal	Interior
Tracheid void volume ($\times 10^{-12}$ m^3)	Earlywood	8.63	4.05
	Latewood	4.49	2.07
Tracheid length (mm)		5	3.5
Tangential width (µm)		40	33
Radial width (µm)	Earlywood	48	39
	Latewood	25	20
Volume ($\times 10^{-7}$ m^3)	REV	2.11	1.12
	Total REV	1.58	0.838
Total ring width (mm)		1.22	1.13
Number tracheids radial direction	Earlywood	14	20
	Latewood	15	9
Earlywood % ring width		59.5	77.3
Latewood % ring width		40.5	22.7
Refilling rate ($\times 10^{-18}$ m^3 s^{-1})		3.03	1.42
No. pits per tracheid	Earlywood	116–180	58–80
	Latewood	90–120	34–60
No. pits per tapered wall	Earlywood	27–35	13–15
	Latewood	20–23	8–10
No. pits per tangential wall	Earlywood	1–6	1–3
	Latewood	0–4	0–2
No. pits per radial wall	Earlywood	1–7	1–3
	Latewood	0–4	0–4
No. pits per ray-tracheid wall	Earlywood	2–6	1–4
	Latewood	2–6	1–4
Bordered-pit K_P (10^{-17} m^3 s^{-1} Pa^{-1})	Earlywood	7.81	7.81
	Latewood	0.391	0.391
Bordered-pit cavitation factor	Earlywood	1	1
	Latewood	0.9	0.9
Tracheid taper fraction		0.1	0.1

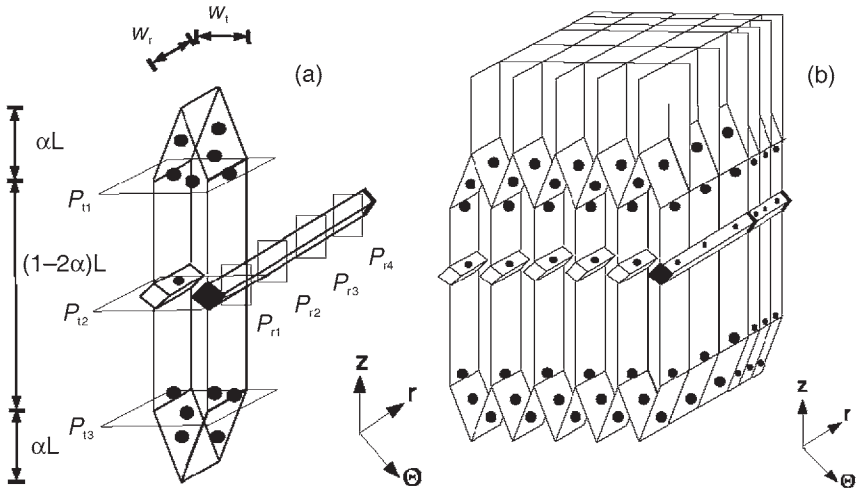

Figure 1. (a) Diagram of a single tracheid and ray tracheid. The pressure within the tracheid is computed at three discrete regions (P_{t1}, P_{t2}, P_{t3}) by applying the principle of mass conservation, as described in the Appendix. Pressures within the ray are also computed at discrete regions P_{r1}–P_{r4}. Abbreviations: α is the tracheid taper fraction; L is the tracheid length; w_r is the radial width; and w_t is the tangential width. (b) Part of the block of tracheids, as represented in the tracheid model. Ray tracheids run radially over a random number of tracheids and the radial width of tracheids decreases between the early (front) and latewood (back). Simulations are done over a block of 45 × 45 × 45 tracheids and variables of interest calculated over a representative elementary volume of 29 × 29 × 29 tracheids. The vertical, radial and tangential directions are denoted by z, r and Ξ, respectively.

Representation of tracheids

Tracheids and rays are represented in the model as shown in Figure 1. Tracheids are assumed to have rectangular cross sections with radial widths differing between earlywood and latewood. Bordered pits in each wall are assumed to have the same dimensions and properties in both coastal and interior earlywood and latewood. The number of bordered pits on each wall is generated according to a uniform distribution with ranges specified in Table 2.

The rays in the model represent the ray tracheids present in gymnosperm wood and enable fluid flow between non-neighboring tracheids. In gymnosperms, ray tracheids are composed of parenchyma cells and ray tracheids which are generally one cell wide and up to 20 cells high (Esau 1965, p 253), but their overall radial length is indeterminate (Esau 1965, p 247). In the model, the ray tracheids connecting tracheids are modeled as a single rectangle with a square cross section, two ray tracheids intersect the sides of each tracheid and each ray intersects a random number of tracheids, ranging from two to four. In coastal wood, the number of bordered pits at each ray tracheid–tracheid intersection ranges between two and six, whereas in interior wood it ranges between one and four (Table 2).

To eliminate the influence of the external boundary, the representative elementary volume (REV) of tracheids (29 × 29 × 29) over which the large-scale variables are computed, is surrounded by a boundary layer of eight tracheids. The size of this boundary layer was determined to be adequate to eliminate the influence of an external boundary (Aumann and Ford 2002*b*). The number of tracheids in the radial direction of the REV represents a growth ring. For coastal wood, the height of the REV is ~13 cm, with a tangential width of ~1.2 mm and a ring width of ~1.0 mm and the corresponding dimensions for interior wood are ~9 cm, ~1 mm and ~0.9 mm. Within the REV, a given number of tracheids is represented as earlywood tracheids and the remainder as latewood tracheids (see Figure 1, Table 2).

Cavitation processes

Cavitation can occur in all tracheids provided that, at the time of cavitation, they are connected vertically to the top and bottom layers of tracheids by a continuous path of uncavitated conducting tracheids. Uncavitated tracheids that are not part of this continuous path of conducting tracheids are assumed not to cavitate. Ray tracheids, which have few bordered pits, are assumed not to cavitate.

When a tracheid cavitates, the volume of water removed is assumed to be 0.6–0.9 of the tracheid's void space volume (Aumann and Ford 2002*b*) and is assumed to be transported away instantaneously by the conducting stream before the bordered pits aspirate. The residual water in the tracheid following cavitation and pit aspiration is assumed to be between 0.1 and 0.4 of the tracheid's void space volume and uniformly distributed. This accounts for the variable amount of water that tracheids contain following cavitation and pit aspiration.

Two separate mechanisms of cavitation are modeled: homogeneous nucleation by adhesion failure and air-seeding through a bordered pit. The model starts with fully saturated tracheids, just as the last formed growth ring is fully saturated at the start of the subsequent season and the first cavitations are assumed to result from homogeneous nucleation. This process is modeled as an inhomogeneous Poisson process (Ripley 1987) in which the rate of cavitation increases with increasing water tension (Aumann and Ford 2002*b*).

Air-seeding occurs when the pressure differential between neighboring cavitated and uncavitated tracheids is larger than the critical pressure required to draw gas through the largest pore in the shared pit tori (Tyree et al. 1994). The process of air-seeding, however, is implemented differently from that described by Aumann and Ford (2002*b*). Here, each bordered pit in each tracheid wall is assigned a random cavitation pressure generated by scaling a Beta(7,1) random variable by the minimum air-seeding pressure of –6.0 MPa which describes Figure 3 of Sperry et al. (1996). Air-seeding from a cavitated to an

uncavitated tracheid through the shared wall occurs when the pressure potential in the uncavitated tracheid is less than the maximum cavitation pressure potential for all the pits in the shared wall. As a result, the cumulative probability of air-seeding increases with absolute pressure potential difference across the shared wall and with increases in the number of bordered pits.

Refilling processes

Each tracheid is connected to one or more rays (Esau 1965, p. 253). In the model, the entire REV is considered to be non-living tissue. According to the PCIX mechanism (Milburn 1996), the water for refilling is water that is freed from the phloem stream when solutes are unloaded. It is assumed that this freed water is transported through the rays to cavitated tracheids.

The refilling rates for coastal and interior wood were chosen so that it takes ~33 days to refill a completely empty coastal or interior earlywood tracheid at the maximum rate of refilling. These rates are approximated from Waring and Running (1978; Figure 3) where it took ~4 months from the end of summer for the relative water content in coastal wood to go from 55% to 100%.

We are unaware of studies suggesting that ray cells direct freed water to particular cavitated tracheids. Thus, the model assumes that such freed water is distributed to all cavitated tracheids by rays, but the rate of flow to tracheids is limited by the rate at which water is freed from the phloem. Thus, maximum refilling rate decreases with decreasing water potential from 100% at 0 MPa to 0% at potentials less than –1.25 MPa to account for the lower flow and diameter contractions associated with such decreased water potentials. The refilling rate per tracheid also decreases linearly from 100% once 25% of the tracheids in the REV are cavitated, to 25% of the original flow value when all tracheids are cavitated. Finally, because the PCIX mechanism is a biological process, it is assumed to stop if the temperature drops below 8 °C.

Flow through the cell wall

It is assumed that the residual water in cavitated tracheids is distributed over the tracheid's slightly permeable walls and that the rate water is drawn out of a cavitated tracheid depends on the amount of wall area shared with neighboring tracheids that are part of the transpiration stream, the pressure differential, cell wall conductivity and cell wall thickness. The manner in which outflow through the cell wall is computed has been described previously (Aumann and Ford 2002*b*).

Driving pressure and time stepping

Our goal was to explore how changes in wood microstructure influence macroproperties of tree water relations under different climate conditions. We assumed that higher maximum daily temperatures correspond to higher transpiration rates and thus higher tensions in the sapwood.

Driving functions are based on daily maximum temperature data from a coastal (Seatac Airport) and interior (Coeur d'Alene) location obtained from http://lwf.ncdc.noaa.gov/oa/climate/climatedata.html. Temperature is used as a surrogate for the suite of variables governing stomatal transpiration rates (Jarvis 1979). Daily data were obtained for 5 years, from January 1, 1997 to January 1, 2002. For day d, let $T_s(d)$ and $T_c(d)$ be the daily maximum temperature for Seatac and Coeur d'Alene, respectively, and let Q_s^{95} and Q_c^{95} be the 95th temperature quantile for the entire maximum daily temperature series. The 95th quantile, instead of the maximum, is used to standardize the two time series because it is a more robust estimate of typical high temperatures. If maximum daily temperature is greater than 8 °C, then the maximum coastal pressure amplitude (Pa) for day d is given as:

$$\left(\frac{-T_s(d)}{Q_c^{95}}\right) 2,500,000 \tag{1}$$

and the maximum interior pressure amplitude (Pa) is given as (Lopushinsky 1986, Bauerle et al. 1999):

$$\left(\frac{-T_c(d)}{Q_c^{95}}\right) 3,000,000 \tag{2}$$

If the maximum daily temperature is less than 8 °C, no transpiration is assumed to occur and the driving potential is zero. To examine the effect of a driving potential between these extremes, a mixed daily pressure amplitude was constructed by averaging the coastal and interior amplitudes for each day.

The tracheid model uses time-steps that are less than an hour, so the pressure amplitude from Equations 1 or 2 is used to scale a sin function with a period of 24 h. Let:

$$t_{\text{val}} = \sin\left(\frac{2\pi}{24t}\right) \tag{3}$$

where t_{val} represents the diurnal cycle and t is time in h. Thus, the driving pressure potential (DPP; Pa) at any time is given by:

$$\text{DPP} = \begin{cases} \text{Amplitude}\,(t_{\text{val}}) & \text{if } t_{\text{val}} \geq 0 \\ 0 & \text{if } t_{\text{val}} < 0 \end{cases} \tag{4}$$

For each day, the pressure potential varies between the minimum given by the amplitude for that day and 0. For the five years of temperature data used, the minimum, 1st quartile, median, 3rd quartile and maximum daily pressures for the coastal driving function are –2.93, –2.15, –1.79, –1.54 and 0 MPa, respectively, and the corresponding values for the interior driving function are –3.42, –2.47, –1.86, 0 and 0 MPa. The coastal values are close to those measured by Bauerle et al. (1999). The interior driving function produces greater tensions, but also has a greater number of days when the maximum tension is 0 MPa because of the longer period of winter conditions at Coeur d'Alene than at Seatac Airport.

The pressure in tracheids in the transpiration stream is set to the driving pressure and changes in the state of tracheids within the block (cavitations, refillings and flow through cell

wall) are calculated over small, variable sized time steps as described by Aumann and Ford (2002*b*). To ensure that important pressure variations are not missed, the largest time step was 1 h.

Computing the macro scale variables

Aumann and Ford (2002*a*) argued that the theory of unsaturated flow through porous media provides a theoretical framework for understanding water flow in trees. The macroscale variables of maximum hydraulic conductivity and the hydraulic conductivity over time are computed as described by Aumann and Ford (2002*b*), but with changes to account for within-tracheid and within-ray-tracheid flow resistance. Potentials or pressures within each tracheid or ray-tracheid are computed at a discrete number of locations (Figure 1). The pressure at each discrete location (e.g., P_{t1}) is found by applying boundary pressure conditions for the top and base of the REV in conjunction with the principle of mass conservation to the flows in or out of each location in the transpiration stream. The boundary pressure at the base is given by the pressure from Equation 4 and the boundary pressure at the top is set to the same value minus a pressure differential of δP (Pa). The flows at each location have associated resistances described in greater detail in the Appendix. Once pressures along the transpiration stream have been found, hydraulic conductivity (K_z; m s^{-1}), is computed by dividing the total volumetric flow (Q; m^3 s^{-1}), through the REV by the cross-sectional flow area (A; m^2) and the δP across the REV (Bear 1972):

$$K_z = \frac{-Q\rho gL}{A\delta P} \quad (5)$$

where L is length of the REV across which δP is applied, ρ (kg m^{-3}) is density of water and g (m s^{-2}) is acceleration due to gravity.

Saturation (m^3 m^{-3}) is defined as the volume of water in the void space of the REV divided by the total volume of the void space and is always between 0 and 1. The void space of the REV is the volume of the REV unoccupied by cell walls. The total residual water (m^3) is the sum of the residual water remaining in just cavitated tracheids comprising a block of wood (earlywood, latewood or the entire REV) and when divided by the void space of the wood gives the residual water per REV void volume. The proportion of cavitated tracheids is the number of cavitated tracheids in a block of wood (earlywood, latewood or REV) divided by the total number of tracheids in the block of wood. Latewood proportion is the proportion of the overall ring width taken up by latewood tracheids.

Results

Model behavior

Figure 2 summarizes the time course of saturation, residual water per REV void volume and proportion of cavitated tracheids for both wood types with tracheid dimensions given in Table 2. Based on these plots, when the response of each ecotype was simulated with its own environmental conditions, it took ~2 years for model dynamics to stabilize. This is because the REV starts fully saturated on January 1, 1997. After the stabilization period, i.e., from January 1999 onward, saturation of coastal wood was generally between 0.7 and 0.8, whereas saturation of interior wood was lower at 0.5–0.6. Generally, the proportion of cavitated coastal tracheids was between 0.2 and 0.3, whereas the proportion ranged between 0.5 and 0.6 for interior wood. Interior wood also had more residual water relative to the void volume comprising its REV than coastal wood.

The maximum vertical hydraulic conductivities for coastal and interior wood were 5.06×10^{-5} and 3.07×10^{-5} m s^{-1}, respectively (Figure 3), values well within measured ranges (Bramhall and Wilson 1971, Markstrom and Hann 1972, Siau

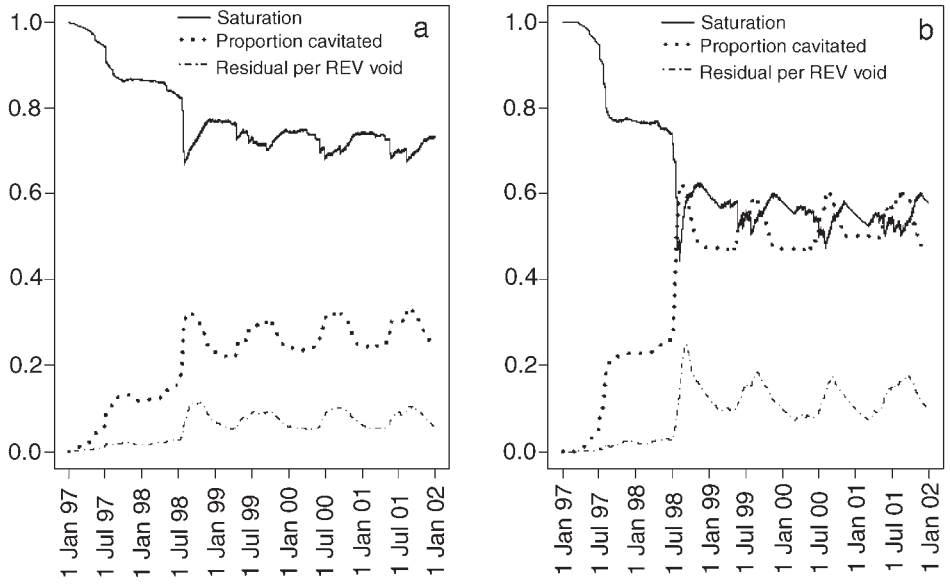

Figure 2. Time course of saturation, residual water per representative elementary volume (REV) void volume (m^3 m^{-3}) and the proportion of cavitated tracheids for coastal (a) and interior wood (b) under their associated driving functions.

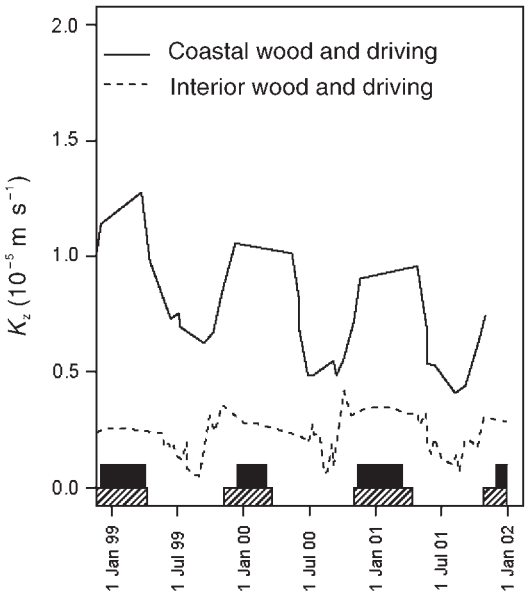

Figure 3. Time course of vertical hydraulic conductivity (K_z) for both coastal and interior wood types under their associated driving functions. Solid bars indicate times when transpiration is not occurring for coastal wood and hatched bars indicate periods when interior wood is non-transpiring.

1995, Spicer and Gartner 2001, Domec and Gartner 2002*a*). Maximum conductivities of the earlywood and latewood were 8.47×10^{-5} and 0.48×10^{-5} m s^{-1} for coastal wood, similar to those reported by Domec and Gartner (2002*a*), and 4.01×10^{-5} and 0.20×10^{-5} m s^{-1} for interior wood.

The ratio of Q in latewood relative to Q in earlywood for coastal and interior wood averaged < 0.05 in the first two summers and was 0.3 and 0.07, respectively, thereafter. Thus, over the first two years, the majority of water flow occurred in the earlywood and water flow in latewood was negligible.

Factors altering maximum conductivity

Figure 4 shows the maximum conductivity for coastal wood when tracheid length, bordered-pit flow constant (K_p; m^3 s^{-1} Pa^{-1}; see Equation A2) and effective tracheid diameter (D_e, see Equation A4) were scaled by a range of factors. The K_p governs how easily water flows through bordered pits, whereas D_e is used to alter the flow resistance in the tracheid lumen. Tracheids of a given diameter may be hydrologically equivalent to tubes with smaller diameter ($D_e < 1$) because of helical thickenings and bending. We used $D_e > 1$ to examine the effect of reducing a tracheid's lumen resistance so that the tracheid is hydrologically equivalent to a larger diameter tracheid. The cross-sectional area of the tracheid is unaltered by changing effective tracheid diameter. Table 3 summarizes the proportional changes in conductivity as these microstructure attributes were altered from the default values (i.e., the solid circle in Figure 4b for coastal wood). Based on the data presented in Figure 4 and Table 3, we were able to identify the attributes primarily responsible for altered maximum conductivity. First, K_p, tracheid length and D_e can all limit vertical conductivity depending on the values used. Second, increasing or decreasing tracheid length or K_p altered K_z in an approximately linear fashion around the default parameter values (Table 3). Third, increasing D_e by a factor of three increased maximum K_z by factors less than 1.12, whereas decreasing the D_e by a third decreased maximum conductivity by factors of 0.56 and 0.68 for coastal and interior wood, respectively (Table 3). Fourth, increasing the actual tracheid diameter (by scaling actual tracheid width and depth in Table 3 rather than effective tracheid diameter) decreased conductivity by a factor of ~0.42, whereas decreasing actual tracheid diameter increased conductivity by factors of 1.27–1.44. In summary, neither tracheid diameter nor D_e limited maximum K_z in coastal or interior wood under the default parameterization, whereas both tracheid length and bordered-pit flow resistance did.

Factors altering conductivity through time

Pit properties A pit's margo and torus are the primary structures governing resistance to water flow through a bordered pit and they also play a direct role in air-seeding, either by facilitating "capillary-seeding" through holes in the pit torus (Sano et al. 1999), "stretch-seeding," "rupture-seeding" (Hacke et al. 2004) or allowing air-seeding through margo pores in unaspirated latewood tracheids (Domec and Gartner 2002*b*). Unfortunately, the relationship between a pit's flow properties and its air-seeding potential are unknown for Douglas-fir. To examine how the uncertainty between ease of flow through the bordered pit and air-seeding potential affects conductivity over time, five K_ps were crossed in a full factorial simulation experiment with five pit cavitation factors for both coastal and inte-

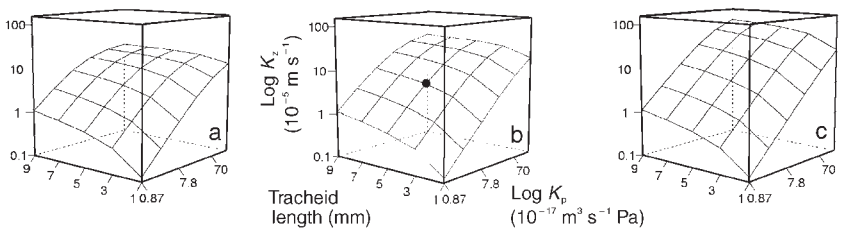

Figure 4. Maximum vertical conductivity (K_z; z axis on log scale) as a function of tracheid length (x axis) and bordered-pit flow constant (K_p; y axis on log scale) conditional on the scaling factor used to scale the effective diameter (D_e, see Appendix) for coastal-like tracheids is 1/2 D_e, D_e and 5/3 D_e for (a)–(c), respectively. The solid circle in panel (b) shows the maximum default conductivity (5.06×10^{-5} m s^{-1}) of a coastal tracheid under the parameters given in Table 2. The graphs indicate that tracheid length, pit flow constant and the effective diameter of the tracheid can all limit vertical conductivity over the parameter ranges considered. Proportional changes in conductivity are given in Table 3.

Table 3. Proportional changes in maximum hydraulic conductivity (K_z; 10^{-5} m s^{-1}) associated with scaling tracheid length, bordered-pit flow constant (K_p), effective tracheid diameter (D_e, see Appendix) and tracheid diameter for coastal and interior wood. All tracheid values are expressed relative to the default values for coastal and interior wood as given in Table 2. Tracheid diameter refers to collectively scaling tangential width, earlywood radial width, latewood radial width and the side-length of the square ray cells.

Factor	Coastal wood	Interior wood
Default maximum K_z (10^{-5} m s^{-1})	5.06	3.07
Tracheid length factor		
0.2	0.22	0.22
0.6	0.63	0.62
1.4	1.33	1.35
1.8	1.64	1.68
K_p *factor*		
1/9	0.12	0.12
1/3	0.36	0.35
3	2.41	2.53
9	4.61	5.22
D_e *factor*		
1/3	0.51	0.58
2/3	0.87	0.90
5/3	1.09	1.06
3	1.12	1.09
Tracheid diameter factor		
1/3	1.27	1.44
3	0.42	0.41

rior wood types. The cavitation factor scales the pressure at which the pits facilitate air-seeding. Factors > 1 increase this pressure (i.e., smaller tension) and facilitate cavitation, whereas values < 1 decrease this pressure. The pit flow constant factors were 0.757, 0.885, 1, 1.100 and 1.190 of the values given in Table 2 for both earlywood and latewood tracheids of both ecotypes. The cavitation factors for earlywood were 0.8, 0.9, 1.0, 1.1 and 1.2, whereas for latewood the factors were 0.7, 0.8, 0.9, 1.0 and 1.1; reflecting the assumption that latewood pits are slightly more resistant to cavitation than earlywood pits. The same cavitation factors were used for both wood ecotypes.

Given that earlywood tracheids were primarily responsible for the overall conductivity of the growth ring in both ecotypes, mean conductivity is plotted relative to the earlywood properties in Figure 5. Clear differences in the functional responses of mean conductivity between the ecotypes were observed. The solid circle and arrows in Figure 5a indicate how changes in K_p and cavitation factor alter mean conductivity. Increasing (or decreasing) a pit's flow constant will likely only increase (or decrease) a pit's cavitation factor, because pits that are less conductive (i.e., greater density of margo fibrils) are less likely to facilitate air-seeding. The arrow pointing toward the back of the graph indicates that decreasing the pit's flow constant and cavitation factor may be associated with increases or decreases in average conductivity depending on the precise relationships between the flow constant and cavitation factor; however, in this case, average conductivity generally increases. Conversely, the arrow pointing toward the front of the figure shows that the average conductivity would likely decrease in response to increases in the pit flow constant and cavitation factor. Given the uncertainty about these properties, regardless of where the solid circle and arrows are located in these figures, the same description applies. Thus, knowing the precise relationship between a bordered pit's flow constant and the associated cavitation factors for a given ecotype are essential for determining whether increases in the rate of flow through the pit are associated with higher or lower average wood conductivity. In summary, although increasing K_p increases maximum hydraulic conductivities, increasing flow through the pit will also increase the air-seeding potential by some degree. The relationship between these properties determines whether mean hydraulic conductivity increases or decreases for each ecotype.

Number of pits × driving functions The maximum K_z can also be increased by increasing the number of bordered pits in a tracheid. However, for mean conductivity to increase, the associated increase in air-seeding potential must be small to avoid counteracting the gains. Three distributions of bordered pits (low, default and high) for both coastal and interior wood types were crossed with three driving function intensities (coastal, mixture and interior). The mean number of low pits is ~0.71–0.87 of the mean default number of pits, whereas the mean number of high pits is ~1.31–1.51 of the default. The actual numbers of bordered pits are given in Table 4. Results are summarized in Table 5 and Figure 6.

Increasing driving function intensity led to larger decreases in saturation and increases in the proportion of cavitated tracheids than increasing the number of bordered pits. For both wood types, saturation was always lower for earlywood than for latewood, whereas the proportion of cavitated tracheids was higher in earlywood than in latewood. Maximum conductivity increased with number of bordered pits (Figure 6), whereas the utility of more pits over time depended on the particular driving function used. During summer under a coastal driving function, more pits led to reduced conductivity for coastal wood and higher conductivity for interior wood. Under a mixed driving function (not shown), increased pits were associated with more rapid declines in conductivity in the first two years (i.e., during the model stabilization period) and lower conductivities during subsequent summers. For interior wood under an interior driving function, increasing the number of pits beyond the default value resulted in a higher rate of decrease in conductivity over the first summer. For more highly pitted coastal wood under an interior driving function, the rate of decline in the first summer was rapid for all three bordered pit distributions. Thus, the "optimal" number of bordered pits for the two wood types depends on the intensity of the driving function.

Exchanging pit distributions between ecotypes The patterns observed in response to altering the number of bordered pits led

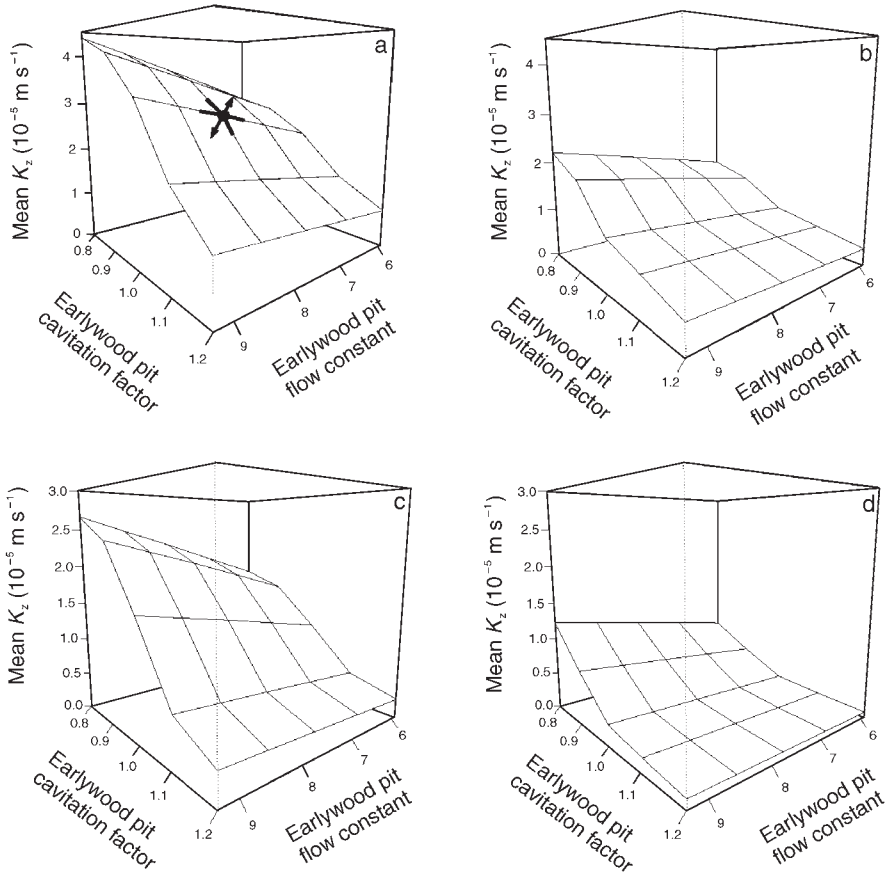

Figure 5. Mean vertical conductivity (K_z) computed for both interior and coastal wood types under their respective driving functions over the summers of 1997–1998 and 1999–2001 as a function of earlywood pit flow constant (10^{-17} m^3 s^{-1} Pa^{-1}) and earlywood cavitation factor. (a) Coastal wood, 1997–1997; (b) coastal wood, 1999–2001; (c) interior wood, 1997–1998; and (d) interior wood 1999–2001. The solid circle (●) and arrows in panel (a) indicate how mean conductivity may change with changes in the pit flow constant and cavitation factor.

us to question what would happen if the number of pits in coastal and interior wood were exchanged and run under either coastal or interior driving functions. This simulation experiment enabled quantification of the extent to which differences in tracheid structure versus number of bordered pits influence the conductivity profile in these ecotypes.

Wood with a coastal wood pit frequency generally had slightly lower saturations and a greater proportion of cavitated tracheids than wood with an interior pit frequency (Table 6). Coastal wood with an interior wood pit frequency had similar maximum earlywood, latewood and REV conductivities as interior wood with an interior wood pit frequency. Likewise, interior wood with a coastal wood pit frequency had similar maximum conductivities to coastal wood with a coastal wood pit frequency (Table 6). As shown in Figure 7, increasing the number of pits led to higher maximum conductivities, but whether a coastal wood pit frequency led to greater conductivity over time depended on the intensity of the driving function. Under a coastal driving function, wood with a coastal wood pit frequency was generally more conductive than wood with an interior wood pit frequency, whereas interior wood with a coastal wood pit frequency was more conductive until July 1998 and generally less conductive during summer than interior wood with an interior wood pit frequency after July 1998 (Figures 7a and 7c). Under an interior driving function, wood with a coastal wood pit frequency was more conductive till July 1997. After July 1998, there was little difference in conductivity, but the variation in conductivity for wood with an interior wood pit frequency was smaller than the variation in wood with a coastal wood pit frequency.

In summary, the maximum conductivity of each wood type was primarily determined by the number of bordered pits and not by tracheid dimensions. Similarly, the differences in conductivity over time between wood types with different pit frequencies were primarily a result of a pit × driving function interaction, not differences in tracheid dimensions. The number of bordered pits in coastal wood resulted in conductivities that were generally highest under a coastal driving function, whereas the number of pits in interior wood gave a conductivity time course that was highest under an interior driving function.

Tracheid length Although increasing tracheid length increased maximum conductivity, the increase only persisted until July 1998 in both coastal and interior wood. After July 1998, the differences in conductivity between shorter and longer tracheids were smaller than those shown in Figures 6–8, because the gains in K_z associated with longer tracheids were negated by increased refilling times.

Refilling rates The conductivity of wood is decreased by cavitation; however, if cavitated tracheids refill, they can rejoin the transpiration stream. Given the uncertainty about whether tracheids refill and, if so, at what rate, four ray refilling rates (none, low, default and high) were modeled for both coastal

Table 4. Changes to the number of bordered pits per tracheid in coastal and interior wood. The pits on each wall are assumed to be uniformly distributed.

Wood type	Coastal wood: pits per tracheid			Interior wood: pits per tracheid		
	Low	Default	High	Low	Default	High
Earlywood	82–136	116–178	158–234	38–60	58–80	82–108
Mean earlywood	109	147	196	49	69	95
Latewood	70–104	88–120	114–158	30–52	34–60	58–84
Mean latewood	87	104	136	41	47	71
Each tapered wall						
Earlywood	20–27	27–35	35–45	8–10	13–15	18–20
Latewood	17–20	20–23	25–30	6–8	8–10	13–15
Each tangential wall						
Earlywood	0–5	1–6	3–10	1–3	1–3	2–5
Latewood	0–4	0–4	2–6	0–2	0–2	1–3
Each radial wall						
Earlywood	0–5	1–7	3–10	1–3	1–3	2–5
Latewood	0–4	0–4	2–6	0–4	0–4	1–5
Each ray-tracheid wall						
Earlywood	1–4	2–6	3–7	1–4	1–4	1–4
Latewood	1–4	2–6	3–7	1–4	1–4	1–4

and interior wood. The default refilling rates were set at 3.03×10^{-18} and 1.42×10^{-18} m^3 s^{-1} for coastal and interior wood, respectively, implying that a completely empty coastal or interior earlywood tracheid would take ~33 days to refill at the maximum refilling rates. High rates were 1.5× higher and low rates were 0.67× lower.

The rate of refilling made little difference to conductivity until July 1998 by which time conductivity had declined by

Table 5. Effects of altering the number of bordered pits on saturation and proportion of cavitated tracheids in coastal and interior wood. The numbers of pits in the low, default and hit pit scenarios are given in Table 4. The effects of number of bordered pits are considered in combination with each driving function. Means were computed over the summers only for years 1999 to 2001. Abbreviation: REV = representative elementary volume.

Wood state	Driving function	Coastal wood: pit frequency			Interior wood: pit frequency		
		Low	Default	High	Low	Default	High
Saturation							
Earlywood	Coast	0.595	0.570	0.553	0.643	0.603	0.579
Earlywood	Mix	0.54	0.535	0.563	0.623	0.566	0.52
Earlywood	Interior	0.553	0.588	0.624	0.518	0.478	0.492
Latewood	Coast	0.983	0.981	0.98	0.955	0.955	0.957
Latewood	Mix	0.965	0.965	0.96	0.89	0.895	0.894
Latewood	Interior	0.92	0.913	0.883	0.833	0.827	0.816
REV	Coast	0.734	0.717	0.706	0.701	0.669	0.65
REV	Mix	0.692	0.689	0.705	0.673	0.627	0.59
REV	Interior	0.684	0.704	0.716	0.577	0.543	0.552
Cavitated							
Earlywood	Coast	0.486	0.541	0.601	0.378	0.429	0.469
Earlywood	Mix	0.594	0.651	0.691	0.411	0.493	0.581
Earlywood	Interior	0.703	0.725	0.742	0.577	0.669	0.704
Latewood	Coast	0.040	0.046	0.048	0.070	0.071	0.071
Latewood	Mix	0.073	0.078	0.092	0.174	0.174	0.185
Latewood	Interior	0.181	0.201	0.288	0.232	0.251	0.302
REV	Coast	0.255	0.285	0.315	0.282	0.318	0.345
REV	Mix	0.325	0.355	0.381	0.337	0.394	0.458
REV	Interior	0.433	0.454	0.507	0.470	0.539	0.579

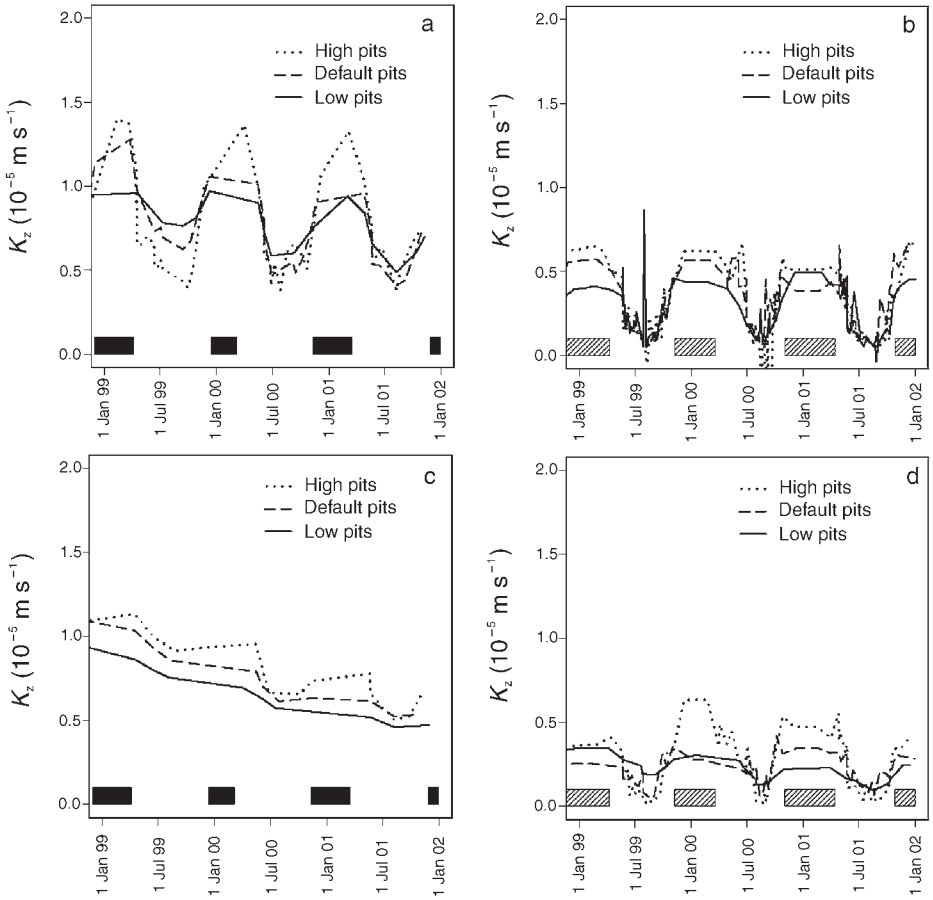

Figure 6. Time courses of vertical conductivity (K_z) for coastal and interior wood containing different numbers of bordered pits under the two driving functions. (a) Coastal wood, coastal driving; (b) coastal wood, interior driving; (c) interior wood, coastal driving; and (d) interior wood, interior driving. The solid and hatched bars indicate the general time periods when transpiration and refilling cease.

more than 90%. Subsequently, conductivities for coastal wood were ordered according to the rate of refilling: High > Default > Low > None, whereas for interior wood the pattern was mixed for Default and Low (Figure 8). With no refilling, conductivity in coastal and interior wood under their respective driving functions reached 10% of their respective maximum values midway through the second summer. Thus, rates of refilling had the greatest effect on the conductivity of wood after the first two summers and had almost no effect before this time.

Percentage of latewood Given the large differences in the percentage of latewood between ecotypes, we examined how the conductivity profiles change as this percentage is altered. The total number of tracheids in the radial dimension was fixed at 29, but the number of latewood tracheids was altered. Low, default and high corresponded to 12, 15 and 18 latewood tracheids in coastal wood (36, 46 and 57% total ring width) and 5, 9 and 13 (13, 23, 35% total ring width) in interior wood. Because the overall dimensions of the REV change with altered percentages of latewood, Q (Equation 5), was used to compare the scenarios.

The ratio of Q with high and low percentages of latewood relative to Q with the default percentage of latewood is shown in Figure 9. From the beginning of 1997 to July 1998, a low percentage of latewood gave flow rates ~1.2× higher than with the default percentage of latewood, whereas with a high percent of latewood flow rates were ~0.8 of the default for both wood types. This general pattern also held after July 1998, although the flow rates showed much greater variability because flow rates decreased dramatically (Figure 9). This result is consistent with the finding that most of the conductivity of the REV is accounted for by the earlywood.

Discussion

Factors controlling sapwood conductivity

Here we consider the following question: How do maximum conductivity and the conductivity time course change when the meteorological driving function, number and conductive properties of bordered pits, tracheid dimensions (length, diameter, effective diameter), tracheid refilling rates and proportion of latewood are altered?

Maximum conductivity The simulations show that tracheid diameter does not limit flow through the wood matrix. First, increasing the effective diameter of tracheids (which is equivalent to decreasing the resistance offered by the tracheid lumen) results in only small increases in maximum K_z (Table 3). Second, increasing the physical dimensions of the tracheid by scaling tracheid width, depth and ray size decreases maximum conductivity, whereas decreasing these dimensions increases

Table 6. Effects of switching the number of pits in coastal wood to the number of pits in interior wood and switching the number of pits in interior wood to the number of pits in coastal wood and running all wood types under coastal and interior driving functions. The numbers of bordered pits per tracheid are given in Table 4 under the default column. Means for saturation and proportion of cavitated tracheids were computed over the summers only for years 1999 to 2001. Abbreviations: K_z = vertical hydraulic conductivity; and REV = representative elementary volume.

	Driving function	Coastal wood: pit frequency		Interior wood: pit frequency	
		Coastal	Interior	Coastal	Interior
Saturation					
Earlywood	Coast	0.57	0.631	0.519	0.602
Earlywood	Interior	0.527	0.523	0.55	0.478
Latewood	Coast	0.981	0.985	0.952	0.954
Latewood	Interior	0.846	0.949	0.812	0.857
REV	Coast	0.717	0.758	0.601	0.668
REV	Interior	0.641	0.676	0.599	0.543
Cavitated					
Earlywood	Coast	0.541	0.425	0.583	0.429
Earlywood	Interior	0.634	0.639	0.732	0.669
Latewood	Coast	0.046	0.035	0.078	0.070
Latewood	Interior	0.393	0.111	0.345	0.251
REV	Coast	0.285	0.223	0.426	0.318
REV	Interior	0.510	0.366	0.612	0.539
K_z (10^{-5} m s^{-1})					
Max earlywood		8.47	4.11	7.97	4.01
Max latewood		0.475	0.2	0.455	0.195
Max REV		5.06	2.45	6.12	3.07

maximum conductivity. This occurs because increasing tracheid diameter alters the *A* of the REV. Because tracheid diameter does not limit flow, increasing tracheid diameter results in essentially the same *Q* over a larger *A*, consequently K_z (Equation 5) decreases. Likewise, decreasing tracheid diameter increases conductivity for the same reason because essentially the same *Q* is occurring through a smaller *A*. Third, the maximum conductivity of interior wood with a coastal wood pit distribution (with smaller diameter tracheids) is larger than that of coastal wood with a coastal wood pit distribution (Table 6). If tracheid diameter is limiting flow in interior tracheids, this would not be the case.

The changes in maximum conductivity that occur in response to altering pit conductivity, number of bordered pits per tracheid and tracheid length are approximately linear and one-to-one (Table 3). The percentage of the growth ring comprising latewood also has an approximately linear effect on the maximum volume of flow through the REV. However, altering K_p, tracheid length, D_e or tracheid diameter indicate that each of these different tracheid properties limit maximum conductivity when these parameters reach extreme values (Figure 4)—a result agreeing with that found by Hacke et al. (2004). In conclusion, attempting to explain differences in maximum K_z solely on the basis of tracheid diameter in the Hagen-Poiseuille equation fails to provide an adequate explanation. The model shows that several microstructure attributes need to be considered to account for differences in maximum K_z.

Hydraulic conductivity over time Because altering attributes to increase maximum conductivity generally decreased mean conductivity, focusing on maximum K_z will not provide a complete understanding of how wood microstructure affects water transport. The effects of altering the microstructure must also be considered over time.

The scenarios revealed several aspects of how wood microstructure affects water transport. First, altering the number of pits within a given wood type (Figure 6) and switching the bordered pit distributions between coastal and interior wood (Figure 7) both show that a pit × driving function interaction primarily determines the conductivity profile over time, not tracheid dimensions. Second, under severe environmental conditions, having pits that are less conductive can be advantageous. Over the range of pit flow constants and air-seeding factors considered, increasing the ease of flow through the pit is mostly associated with increases in pit air-seeding and hence decreases in mean conductivity: it is only associated with increases in mean conductivity if the associated increases in pit air-seeding are small (Figure 5). Although pit encrustations likely increase the flow resistance through the pit, if encrustations also reduce the potential for air-seeding they could increase mean conductivity (Figure 5) under severe driving conditions and thus be beneficial. Finally, although increasing tracheid length and refilling rate increase maximum K_z, increasing tracheid length only increases conductivity over the first 1.5 summers (after which no dramatic differences are evident), whereas increasing ray refilling rate only affects the conductivity profile after the first two years.

In conclusion, altering attributes to increase maximum conductivity generally lead to lower conductivity over time. Of

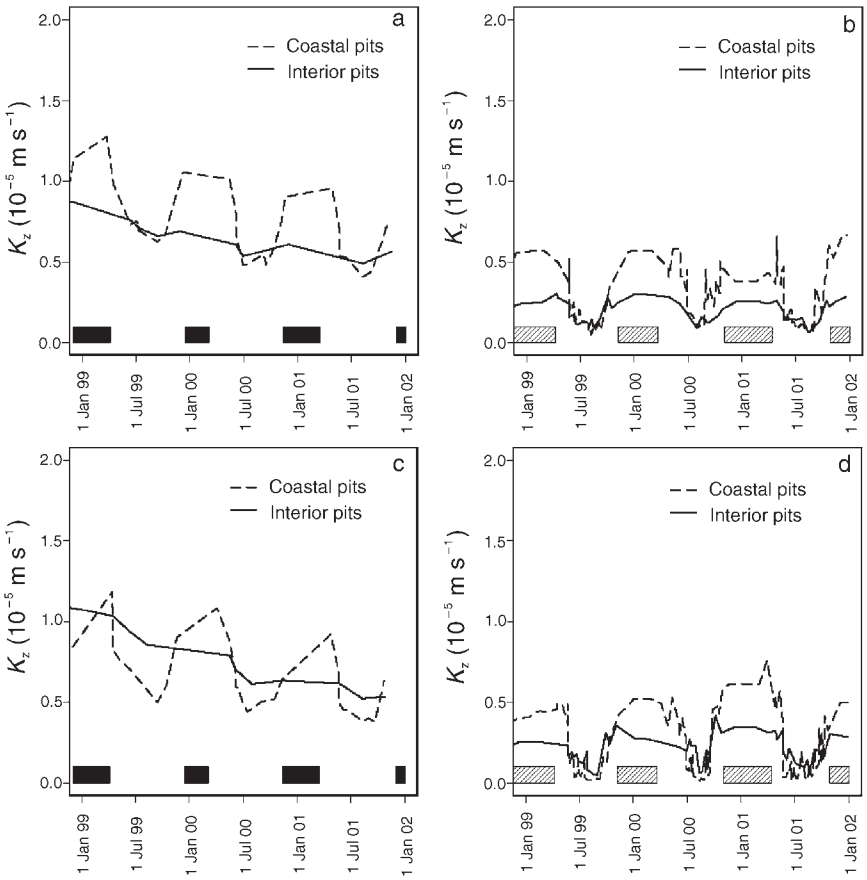

Figure 7. Time courses of vertical conductivity (K_z) for coastal and interior wood after switching the pit distributions between wood types. (a) Coastal wood, coastal driving; (b) coastal wood, interior driving; (c) interior wood, coastal driving; and (d) interior wood, interior driving. The solid and hatched bars indicate the general time periods when transpiration and refilling cease.

the attributes considered, the number of bordered pits and their associated conductive and air-seeding properties show the largest effects on the conductivity profile over time.

Natural relection and sapwood conductivity

Finally, we consider the following question: Given the differing effects of altering tracheid attributes on conductivity, which attributes may have been the focus of natural selection?

Bordered pits Fewer pits that are also less conductive because of pit encrustations provide a less variable supply of water to the foliage (Figure 7). This can be beneficial in interior Douglas-fir because Douglas-fir stomata are relatively insensitive to water stress (Stout and Sala 2003). The results in Figure 7 suggest that, under less severe driving functions, selective pressures would favor a greater number of more conductive bordered pits, whereas it would favor fewer and less conductive pits under more severe conditions. Another possibility is that selection operates for maximum plasticity in the number and properties of pits based on environmental conditions. The benefit from a strategy that alters pit frequency and pit properties in response to environmental conditions could be large (Figures 6 and 7). Unfortunately, although it is known that pit morphology is highly variable across gymnosperms (Bauch et al. 1972), we are unaware of studies on how the number of bordered pits or their morphological properties change with environmental conditions within and between species.

Tracheid dimensions Tracheid length varies with tree height in Douglas-fir and in other conifers (Lee et al. 1916, Bannan 1964, Panshin and de Zeeuw 1980). However, unlike the number and properties of bordered pits, the extent to which tracheid length can be altered on a yearly basis is likely limited. Over a longer time frame, selection pressures might favor longer, smaller diameter tracheids because tracheid diameter does not limit flow near the default parameter values considered. One advantage of small diameter tracheids is that they reduce frost-induced embolisms (Tyree et al. 1994, Pittermann and Sperry 2003). Altering tracheid dimensions will also likely alter the strength properties and amount of energy required to construct a unit volume of wood. However, this model cannot predict such wood properties. Snodgrass and Noskowiak (1968) found the specific gravity of coastal sapwood was 2% greater than that of interior wood, assuming that cell walls of coastal and interior wood have the same density, implying that constructing a unit volume of coastal wood requires slightly more energy than constructing a unit volume of interior wood. However, interior wood is also generally weaker than coastal wood (Snodgrass and Noskowiak 1968, Hesterman and Gorman 1992). Thus, selective pressures resulting from conductivity, freeze-induced embolism and wood strength are not likely acting in the same direction on tracheid dimensions.

Refilling rate This model cannot assess the overall costs and benefits of increasing or decreasing the rate of refilling. Ac-

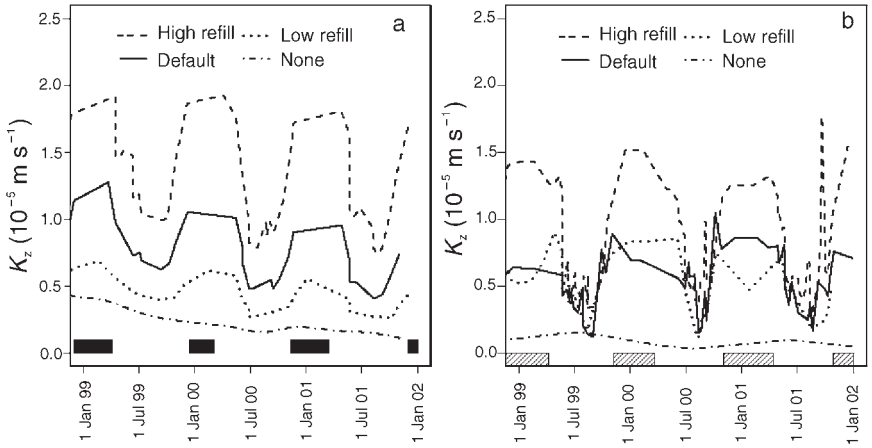

Figure 8. Time courses of vertical conductivity (K_z) for coastal and interior wood types as a function of tracheid refilling rate. (a) Coastal wood, coastal driving; and (b) interior wood, interior driving. The solid and hatched bars indicate the general time periods when transpiration and refilling cease.

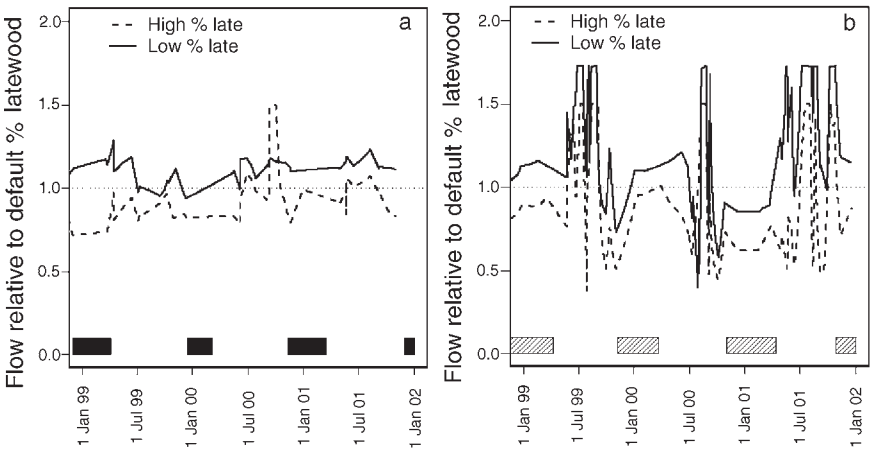

Figure 9. Time courses of volumetric flow in the representative elementary volume (REV) under high and low percentages of latewood divided by the volumetric flow in the REV under the default percentage of latewood. (a) Coastal wood, coastal driving; and (b) interior wood, interior driving. The solid and hatched bars indicate the general time periods when transpiration and refilling cease.

cording to the PCIX mechanism (Milburn 1996), refilling rate could be increased by increasing the volumetric rate of flow in the phloem. But given the small influence refilling rate had on conductivity during 1997–1998 and the many processes involved in PCIX refilling, selection pressures for higher refilling rates are likely small. If conductivity depended heavily on refilling rate, then the more extreme water potentials and drought conditions would require, under the PCIX mechanism of refilling, that interior wood transport a higher volume of sap containing a lower concentration of carbohydrate in the phloem to maintain stomatal conductance. Further, any conditions that disrupted this refilling, such as a seasonal drought, would lead to marked decreases in conductivity and likely mortality. Thus, the advantages of conductivity in the sapwood being almost independent from refilling rate over the first two years are clear.

Amount of latewood Increasing the percentage of latewood decreases the volumetric rates of flow over time, whereas decreasing the proportion of latewood increases flow rates (Figure 9). Given that decreasing the percentage of latewood affects both wood strength and conductivity, the selection pressure to minimize latewood formation and thereby increase conductivity is unclear. Empirically, coastal wood has a higher percentage of latewood than the less conductive interior wood; however, this may simply be the result of the longer growing season for coastal Douglas-fir than for interior Douglas-fir (Kavanagh et al. 1999).

In conclusion, the features most likely to be the focus of natural selection to increase K_z are the number and properties of bordered pits, but it is unclear whether the selection pressures are directed at the number and properties of the pits, or at possible mechanisms allowing the tree to respond plastically to different environmental conditions.

What major uncertainties remain?

This study highlights the importance of increased knowledge about bordered pits for understanding the conductive properties of wood. Of all the factors considered, the number and properties of bordered pits have the largest effect on conductivity and, unlike traits such as tracheid length, should be the easiest to change in response to varying environmental conditions. Unfortunately, because of the inherent difficulties in studying such small entities, bordered pits are not well understood. Several specific questions need to be examined. (1) Is variation in the number and properties of bordered pits related to environmental conditions? (2) Is variation in tracheid dimensions related to variation in bordered pits? (3) How do pit

properties relate to the pit's flow properties and the probability of air-seeding and how do these relationships change with pit morphological variation within and between species?

Although the first two questions need to be answered empirically, the last will require a detailed model capable of relating changes in pit structure (e.g., different diameters and depths of the pit aperture; density, size and number of the margo fibrils; regular versus irregular mesh arrangements of the fibrils; existence and degree of fibril encrustations; modulus of elasticity of the fibrils; pit membrane diameter; diameter of the central torus, etc.) to both flow through the pit and its air-seeding potential. This model must be capable of representing variation in the attributes of a bordered pit (Bauch et al. 1972, Yang and Benson 1997) if the effects of this variation within and between species are to be understood. As a result, computational techniques like the Lattice-Boltzmann method will be required to compute pit conductivity (Valli et al. 2002) and other computational techniques will be needed to quantify air-seeding potential. The resulting relationship between pit conductivity and air-seeding potential can then be used in models like our tracheid model to quantify effects on both maximum and mean conductivity.

Acknowledgments

Detailed comments provided by Dr. Peter Becker and the reviewers led to substantial improvements in both the model and the paper. This research was funded by the Andrew W. Mellon Foundation.

References

Aumann, C.A. and E.D. Ford. 2002*a*. Modeling water flow as an unsaturated flow through a porous medium. J. Theor. Biol. 219: 415–429.

Aumann, C.A. and E.D. Ford. 2002*b*. Parameterizing a model of Douglas fir water flow using a tracheid level model. J. Theor. Biol. 219:431–462.

Bailey, P.J. and R.D. Preston. 1969. Some aspects of softwood permeability. Holzforschung 23:113–120.

Bannan, M.W. 1964. Tracheid size and anticlinal divisions in the cambium of *Pseudotsuga*. Can. J. Bot. 42:603–631.

Bauch, J., W. Liese and R. Schultze. 1972. The morphological variability of the bordered pit membranes in gymnosperms. Wood Sci. Technol. 6:165–184.

Bauerle, W.L., T.M. Hinckley, J. Čermák and J. Kučera. 1999. The canopy water relations of old-growth Douglas fir trees. Trees 13: 211–217.

Bear, J. 1972. Dynamics of fluids in porous media. American Elsevier, New York, 769 p.

Becker, P. and R.J. Gribben and P.J. Schulte. 2003. Incorporation of transfer resistance between tracheary elements into hyraulic resistance models for tapered conduits. Tree Physiol. 23:1009–1019.

Blevins, R.D. 1992. Applied fluid dynamics handbook. Krieger Publishing, Malabar, FL, 558 p.

Borghetti, M. and G.G. Vendramin. 1987. Seasonal changes of soil and plant water relations in Douglas fir forest. Acta Oecol. Oecol. Plant. 8:113–126.

Bramhall, G. and J.W. Wilson. 1971. Axial gas permeability of Douglas-fir microsections dried by various techniques. Wood Sci. Technol. 3:223–230.

Carlquist, S. 2001. Comparative wood anatomy. Springer-Verlag, Heidelberg, 2nd Edn, 448 p.

Chalk, L. and J.M. Bigg. 1956. The distribution of moisture in the living stem in Sitka spruce and Douglas fir. Forestry 29:5–21.

Cote, W.A., Jr. 1967. Wood ultrastructure: an atlas of electron micrographs. University of Washington Press, Seattle, WA, 25 p.

Domec, J. and B.L. Gartner. 2002*a*. Age- and position-related changes in hydraulic versus mechanical dysfunction of xylem: inferring the design criteria for Douglas-fir wood structure. Tree Physiol. 22:91–104.

Domec, J.-C. and B.L. Gartner. 2002*b*. How do water transport and water storage differ in coniferous earlywood and latewood. J. Exp. Bot. 53:2369–2379.

Esau, K. 1965. Plant anatomy. 2nd Edn. John Wiley and Sons, 767 p.

Ferrell, W.K. and E.S. Woodward. 1966. Effects of seed origin on drought resistance of Douglas fir (*Pseudotsuga menziesii*) (Mirb.) Franco. Ecology 47:499–503.

Griffin, B.J. 1919. Bordered pits in Douglas fir: a study of the position of the torus in mountain and lowland specimens in relation to creosote penetration. J. For. 7:813–811.

Hacke, U.G., J.S. Sperry and J. Pitterman. 2004. Analysis of circular bordered pit function. II. Gymnosperm tracheids with torus-margo pit membranes. Am. J. Bot. 91:386–400.

Hart, C.A. and R.J. Thomas. 1967. Mechanism of bordered pit aspiration as caused by capillarity. For. Prod. J. 17:61–68.

Hesterman, N.D. and T.M. Gorman. 1992. Mechanical properties of laminated veneer lumber made from interior Douglas-fir and lodgepole pine. For. Prod. J. 42:69–73.

Holbrook, N.M. and M.A. Zwieniecki. 1999. Embolism repair and xylem tension: do we need a miracle? Plant Physiol. 120:7–10.

Jane, F.W. 1956. The structure of wood. A&C Black, London, 427 p.

Jarvis, P.G. 1979. Stomatal conductance, gaseous exchange and transpiration. *In* Plants and Their Atmospheric Environment. Eds. J. Grace, E.D. Ford and P.G. Jarvis. Blackwell Scientific Publications, Oxford, U.K., pp 175–204.

Kavanagh, K.L., B.J. Bond, S.N. Aitken, B.L. Gartner and S. Knowe. 1999. Shoot and root vulnerability to xylem cavitation in four populations of Douglas fir seedlings. Tree Physiol. 19:31–37.

Krahmer, R.L. 1961. Anatomical features of permeable and refractory Douglas fir. For. Prod. J. 11:439–441.

Lancashire, J.R. and A.R. Ennos. 2002. Modeling the hydrodynamic resistance of bordered pits. J. Exp. Bot. 53:1485–1493.

Lee, H.N., A.M. Smith and E.M. Smith. 1916. Douglas fir fiber, with special reference to length. For. Q. 14:671–695.

Lopushinsky, W. 1986. Seasonal and diurnal trends of heat pulse velocity in Douglas fir and Ponderosa pine. Can. J. For. Res. 16: 814–821.

Markstrom, D.C. and R.A. Hann. 1972. Seasonal variation in wood permeability and stem moisture content of three rocky mountain softwoods. USDA Forest Service Research Note RM-212 (RM-212), 7 p.

Meyer, R.W. 1971. Influence of pit aspiration on earlywood permeability of Douglas fir. Wood Fiber Sci. 2:328–339.

Milburn, J.A. 1975. Pressure flow. *In* Transport in Plants. Encyclopedia of Plant Physiology. Vol. 1. Eds. M.H. Zimmermann and J.A. Milburn. Springer-Verlag, Berlin, pp 328–366.

Milburn, J.A. 1979. Water flow in plants. Longman, London, 255 p.

Milburn, J.A. 1996. Sap ascent in vascular plants: challengers to the Cohesion theory ignore the significance of immature xylem and the recycling of Münch water. Ann. Bot. 78:399–407.

Miller, D.J. 1969. Permeability of Douglas fir in Oregon. For. Prod. J. 11:14–16.

Palin, M.A. and J.A. Petty. 1981. Permeability to water of the cell wall material of Spruce heartwood. Wood Sci. Technol. 15:161–169.

Palin, M.A. and J.A. Petty. 1983. Permeability to water of the wood cell wall and its variation with temperature. Wood Sci. Technol. 17: 187–193.

Panshin, A.J. and C. de Zeeuw. 1980. Textbook of wood technology. McGraw-Hill Books, 722 p.

Pharis, R.P. and W.K. Ferrell. 1966. Differences in drought resistance between coastal and inland sources of Douglas fir. Can. J. Bot. 44:1651–1659.

Phillips, N.G., M.G. Ryan, B.J. Bond, N.G. McDowell, T.M. Hinckley and J. Čermák. 2003. Reliance on stored water increases with tree size in three species in the Pacific Northwest. Tree Physiol. 23:237–245.

Pittermann, J. and J. Sperry. 2003. Tracheid diameter is the key trait determining the extent of freezing-induced embolism in conifers. Tree Physiol. 23:907–914.

Ripley, B.D. 1987. Stochastic simulation. John Wiley and Sons, Hoboken, NJ, 237 p.

Sano, Y., Y. Kawakami and J. Ohtani. 1999. Variation in the structure of intertracheary pit membranes in *Abis sachalinensis*, as observed by field-emission scanning electron microscopy. IAWA J. 20: 375–388.

Siau, J.F. 1995. Wood: influence of moisture on physical properties. Department of Wood Science and Forest Products, Virginia Polytechnic Inst. and State Univ., VA, 227 p.

Snodgrass, J.D. and A.F. Noskowiak. 1968. Strength and related properties of Douglas fir from mill samples. Tech. Rep. 10, Bulletin of the Oregon Forestry Research Lab, 40 p.

Sperry, J.S. and U.G. Hacke. 2004. Analysis of circular bordered pit function I. Angiosperm vessels with homogeneous pit membranes. Am. J. Bot. 91:369–385.

Sperry, J.S., N.Z. Saliendra, W.T. Pockman, H. Cochard, P. Curiziat, S.D. Davis, F.W. Ewers and M.T. Tyree. 1996. New evidence for large negative xylem pressures and their measurement by the pressure chamber method. Plant Cell Environ. 19:427–436.

Spicer, R. and B.L. Gartner. 2001. The effects of cambial age and position within the stem on specific conductivity in Douglas fir *Pseudotsuga menziesii* sapwood. Trees 15:222–229.

Stout, D.L. and A. Sala. 2003. Xylem vulnerability to cavitation in *Pseudotsuga menziesii* and *Pinus ponderosa* from contrasting habitats. Tree Physiol. 23:43–50.

Tyree, M.T. and F.W. Ewers. 1991. The hydraulic architecture of trees and other woody plants. New Phytol. 119:345–360.

Tyree, M.T., S.D. Davis and H. Cochard. 1994. Biophysical perspectives of xylem evolution: is there a tradeoff of hydraulic efficiency for vulnerability to dysfunction? IAWA J. 15:335–360.

Valli, A., A. Coponen, T. Vesala and J. Timonen. 2002. Simulations of water flow through bordered pits of conifer xylem. J. Stat. Phys. 107:121–141.

Waring, R.H. and S.W. Running. 1978. Sapwood water storage: its contribution to transpiration and effect upon water conductance through the stems of old-growth Douglas fir. Plant Cell Environ. 1:131–140.

Yang, K.C. and C. Benson. 1997. Ultrastructure of pits in *Pinus banksiana* Lamb. Wood Sci. Technol. 31:153–169.

Appendix

To avoid computing the continuous pressure function within each tracheid of the representative elementary volume (REV) (which because of the numerous inlets/outlets would rapidly become computationally onerous), the pressure is only computed at particular discrete locations (Figure 1) for the uncavitated tracheids that are part of the transpiration stream. The three locations in a tracheid correspond to the top and bottom (i.e., just before the tracheid begins to taper) and middle of the tracheid (where the ray-cell pits are located). At each discrete location, mass balance is applied over the flows in and out of each discrete unit:

$$\sum Q_p + \sum Q_w + \sum Q_{loc} = 0 \tag{A1}$$

For tracheids and rays, the flows in and out of each location can occur from bordered pits (Q_p), cell walls (if the neighboring tracheid sharing the wall is cavitated and contains residual water) (Q_w) and between locations (i.e., P_{t1} to P_{t2}) (Q_{loc}). We discuss each of these terms with reference to P_{t1}. Other locations are analogous. Given equations linking the pressure drop to the volumetric flow rate for each of the terms in Equation A1, the sparse linear matrix system enabling solution for the unknown P values can be setup analogously to that detailed in Aumann and Ford (2002*b*, Appendix A).

Bordered pits

Valli et al. (2002) used the lattice-Boltzmann method to simulate flow through the bordered pits of conifers. The volumetric flow through a pit can be related to the pressure drop δP_p (Pa) across the bordered pit:

$$Q_p = \frac{-\pi a^3 \delta P_p}{2C\mu} = -K_p \delta P_p \tag{A2}$$

where Q_p ($m^3\ s^{-1}$) is volumetric flow rate through the pit, a is diameter of the pit aperture, μ ($kg\ m^{-1}\ s^{-1}$) is viscosity and C is a constant. With and without the margo present in their model of a *Tsuga canadensis* (L.) Carrière pit, C was estimated as 6693 and 4128, respectively, corresponding to a pit flow constant (K_p) of 3.905×10^{-17} and 6.33×10^{-17} ($m^3\ s^{-1}\ Pa^{-1}$). Using these values in the model of coastal Douglas-fir wood results in earlywood conductivities that are too low and latewood conductivities that are too high based on the values reported by Domec and Gartner (2002*a*). Instead, the values of K_p in Table 2 for earlywood and latewood, 7.81×10^{-17} and 0.391×10^{-17} ($m^3\ s^{-1}\ Pa^{-1}$) are used for both coastal and interior wood. The earlywood value is about 7.5 times smaller than the value found by Lancashire and Ennos (2002) using a scaled physical model of a bordered pit. Setting the pit flow constant for coastal earlywood to 5.88×10^{-16} and for coastal latewood to 0.391×10^{-17} ($m^3\ s^{-1}\ Pa^{-1}$) gives a maximum conductivity for the REV of 20.3×10^{-5} ($m\ s^{-1}$). When the effective diameter factor is set at $2/3$, maximum conductivity is still 12.4×10^{-5} ($m\ s^{-1}$). Given the large variation in conifer pits (Bauch et al. 1972, Yang and Benson 1997), we conclude that the pit flow constant, K_p, is likely species specific.

Cell-walls

Because the pressures are being found only at discrete locations, outflow through the tracheid wall from neighboring

cavitated tracheids has to be partitioned between the three tracheid locations. Any such wall area (A_w) above P_{t1} is thus incorporated into the pressure calculation at P_{t1}, whereas the area between P_{t1} and P_{t3} is incorporated into the calculation at P_{t3}. Volumetric flow rate through the cell wall is calculated as described by Aumann and Ford (2002*b*) using a cell wall conductivity $K_w = 2.25 \times 10^{-19}$ (m s^{-1}) for the different earlywood and latewood cell wall thicknesses (Table 2). Flow through the wall is given by:

$$Q_w = \frac{-A_w K_w (P_{t1} - P_c)}{\rho g L_w} \quad \text{(A3)}$$

where P_c is pressure in the neighboring cavitated tracheid (assumed atmospheric), ρ (kg m^{-3}) is density of water, g (m s^{-2}) is acceleration due to gravity and L_w is wall thickness (Table 2).

Flow between locations

In the case of P_{t1}, the only other location flow can occur to is P_{t2}. Volumetric flow through a rectangular tube (tracheid or ray) with width w and depth d ($d \leq w$) can be expressed as a function of the pressure drop across the tube (Blevins 1992, Table 6.2):

$$Q_{loc} = \frac{-2D^2 wd}{\mu f_{Re}} \frac{P_{t1} - P_{t2}}{L} \quad \text{(A4)}$$

where:

$$f_{Re} = \frac{64}{\frac{2}{3} + \frac{11d}{24w}\frac{2-d}{w}} \quad \text{(A5)}$$

and L (m) is the distance between the two locations and the effective diameter (D; m) is given by:

$$D = D_e \frac{2wd}{w + d} \quad \text{(A6)}$$

where D_e is effective the diameter factor used (e.g., Table 3). This factor enables assessment of how over- or underestimating the effective diameter alters vertical conductivity. The widths and depths are given in Table 2.

To compensate for not modeling flow resistance in the tapered parts of the model tracheid, we used a small tracheid taper fraction ($\alpha = 0.1$ in Figure 1) and located all tracheid pits (excluding pits between tracheids and ray cells) where the tracheid begins to taper. Thus, the flow path is 0.8 of the tracheid's length. Because almost all pits are located at the respective ends of this flow path (Figure 1a, Table 4), any resistance offered by the tracheid lumen will be greater than if the flow path were only 0.5 of the tracheid's length or the pits were distributed uniformly over the tracheid's walls.